Fabrication and Characterization of Polyolefin Filaments for Fused Filament Fabrication

M. Amirulhusni M.Fadzir

Anika Zafiah M. Rus

Yazid Saif

M. Akmal Abd Rabbi

他

https://doi.org/10.5109/7395563

出版情報：Proceedings of International Exchange and Innovation Conference on Engineering & Sciences (IEICES). 11, pp.510-517, 2025-10-30. International Exchange and Innovation Conference on Engineering & Sciences
バージョン：

Fabrication and Characterization of Polyolefin Filaments for Fused Filament Fabrication

M. Amirulhusni M.Fadzir 1, Anika Zafiah M. Rus[1*], Yazid Saif1[2], M. Akmal Abd Rabbi[2], M. Ibrahim[2], M. Zulfadzli Md Zahri[2]
[1]GD240012@student.uthm.edu.my, [2]Yazeedalkosa@gmail.com, [2]HD230023@student.uthm.edu.my,
[2]mustaffa@uthm.edu.my, [2]GD230015@studemt.uthm.edu.my.
Corresponding author email: zafiah@uthm.edu.my

Abstract: *Addressing the urgent need for sustainable and high-performance materials in 3D printing this study pioneers the development of bio-epoxy (BE)-modified low-density polyethylene (LDPE) filaments for fused filament fabrication (FFF) utilizing bio-epoxy derived from waste vegetable oil to enhance mechanical and thermal properties while reducing environmental impact. Mechanical, thermal, and morphological properties were analyzed to identify the optimal formulation.LB 3 exhibited the best performance, with a 4.14% increase in tensile strength 8.819 MPa over unmodified LDPE (8.469 MPa), attributed to enhanced interfacial bonding and uniform filler dispersion. At higher BE loading 5 wt% phase separation and increased surface roughness led to a decline in mechanical integrity. Fractographic analysis showed ductile failure modes across all BE-modified samples, with LB 3 demonstrate superior energy dissipation and crack resistance. Thermal analysis revealed that while BE slightly reduced the onset degradation temperature 180–185°C LB 3 showed the highest thermal stability with a maximum degradation temperature of 486°C. Minimal moisture uptake and consistent filament diameters within 1.70 to 1.75 mm confirmed good dimensional stability. Overall, LB 3 formulation enhanced mechanical strength, thermal resistance, and printability, demonstrate the promise of bio-based fillers in producing sustainable, high-performance filaments for additive manufacturing.*

Keywords: Sustainable material, Bio-epoxy, Low-Density Polyethylene, Fused Filament Fabrication, 3D Printing

1. INTRODUCTION

Polyethylene (PE) a high-volume thermoplastic polymer widely recognized for its cost efficiency and multifunctionality across various industrial sectors such as packaging, agriculture, and biomedical applications. However, the increased production has been associated with a significant accumulation of polymeric waste. PE extensively utilized in flexible packaging and fluid transport systems has been reported to account for 78 million metric tons constitute approximately 20% of global polymer output. This production volume has continued to rise due to the growing demand for lightweight and durable polymeric materials [1]. From a structural standpoint, PE is categorized into different grades based on its branches architecture includes high-density polyethylene (HDPE), low-density polyethylene (LDPE), and linear low-density polyethylene (LLDPE) tabulated in (Fig.1) [2]. LDPE is characterized by a higher density of long-chain branching (8–40 per 1,000 carbon atoms) which disrupts molecular symmetry and results in a reduced crystallinity of 40% to 50% compared to HDPE [3]. This structural irregularity leads to limitations in mechanical strength thermal stability and resistance to stress and deformation.

The application additive manufacturing (AM) is utilized as a layer-by-layer fabrication process where materials are integrated through fusion, binding, or solidification. Precise geometric control and complex architectures are achieved using 3D CAD modeling. Recent advancements have made cost-effective 3D printing systems widely accessible in research, academia, and domestic applications [4]. With this accessibility, the fabrication of multi-material structures with tailored mechanical, thermal, and electrical properties has been facilitated. Conventional methods render such integration costly due to extensive post-processing whereas AM provides a rapid, cost-efficient prototyping platform [5]. The highest manufacturability and scalability for product fabrication have been demonstrated by thermoplastic filament extrusion known as fused deposition modeling (FDM) among various additive manufacturing (AM) techniques [6,7]. Although a diverse range of thermoplastic materials is available for FDM, acrylonitrile butadiene styrene (ABS), polylactic acid (PLA), and polyamide (PA) are most commonly employed [8].

Currently, limited attention has been given to the 3D printing of semicrystalline polymers filament due to its inherent limitations. Semicrystalline polymers are typically subjected to substantial volumetric contraction during the solidification phase following the molten state, as polymeric chains tend to reorganize into a long-range ordered crystalline structure upon deposition onto the print substrate. These polymers are highly prone to excessive warpage and inadequate interfacial adhesion with the print bed significantly compromises print fidelity and structural integrity leads to fabrication defects and process failure [9,10]. Moreover, LDPE's low elastic modulus poses challenges for 3D printing, as it can lead to filament buckling during extrusion. The insufficient rigidity of the solid filament section fails to withstand the stresses required for smooth extrusion through the nozzle. Additionally, poor layer adhesion and a high coefficient of thermal expansion (CTE) contribute to significant shrinkage and warping, compromising the dimensional stability of printed parts [10-12]. These thermal and structural limitations hinder the production of high-quality 3D-printed objects using LDPE-based filaments.

For some years, a single polymer alone does not possess all the necessary characteristics. Some economists agree with this view and share similar perspectives. The concept of formulation has been widely recognized across various industries, where intermediates or finished

products are created by combining multiple raw materials [13]. Composite materials are made by combining two or more different materials to create a final product with improved properties. The synergistic interaction of these materials is enabled by each component, which contributes to enhancing mechanical strength, flexibility, or specific functional attributes. [14,15]. To address the limitations of LDPE, various filler formulations have been explored for example LDPE/biochar composites (90/10 wt%) were studied to enhance the mechanical, thermal, and tribological properties of LDPE. Tensile strength (1.9%), flexural strength (47%), and hardness (24.3%) improved with biochar incorporation without compromising processability. Furthermore, thermogravimetric analysis (TGA) confirmed enhanced thermal stability, while melt flow index (MFI) results indicated reduced flowability. FESEM analysis revealed a well-dispersed biochar morphology, contributing to improved interfacial adhesion. Tribological tests showed a 56.3% reduction in the friction coefficient for LDPE+10 wt% biochar, highlighting its potential as a cost-effective, sustainable filler for high-performance LDPE bio composites [16]. As environmental sustainability gains prominence, extensive research was conducted on hybrid materials to replace conventional, non-eco-friendly composites. In this study, polymeric composites were developed by incorporates waste cooking oil (WCO) as a functional filler and a LDPE is a matrix at variety mass fractions (1, 2, 3, 4, and 5 wt%). The effects of WCO incorporation on the physical, mechanical, morphological, and thermal characteristics of 3D-printable filaments were systematically examined. The primary objective was to fabricate filaments using LDPE and WCO as a filler sourced from small and medium enterprises (SMEs) without additional pre-treatment, thereby reducing defects such as melt fracture and phase separation during extrusion. For each composition, filaments with a length of up to 1.0 meter were successfully extruded.

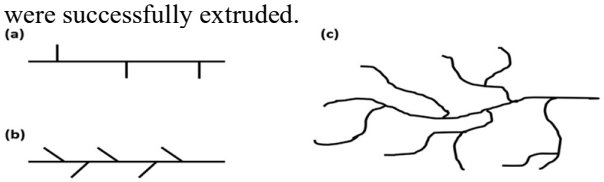

Fig. 1. Structural variations among different grades of PE: (a) High-Density Polyethylene (HDPE), (b) Low-Density Polyethylene (LDPE), and (c) Linear Low-Density Polyethylene (LLDPE).

2. EXPERIMENTAL PROCEDURE

2.1 Material

In this study, the materials utilized for sample fabrication are detailed in Table 1. The polymer matrix consists of LDPE with a density of 0.922 g/cm³ a melt flow index of 4 g/10 min, and a Vicat softening temperature of 124°C. The melting temperature of LDPE ranges between 105-110°C. Additionally, Isocyanate was incorporated exhibit a viscosity of 120-160 cps at 25°C, a specific gravity of 1.18-1.20 g/ml at 25°C. The monomer component was synthesized from waste vegetable oils through an in-house catalytic conversion process facilitating epoxy formation from unsaturated fatty compounds. The condensation process includes formation of hydroxylated monomer by acid-catalysed ring-opening of the epoxides. The hydroxylated monomer was then reacted with the cross-linking agents to produce polymer, namely as bio-epoxy (BE). BE was employed as a functional filler within the LDPE matrix to enhance the mechanical and physical properties of LDPE. The composite filament was fabricated using a Felfill Evo 3 single-screw extruder produced 1.75 ± 0.05 mm diameter filament for 3D printing applications.

Table 1. Material Functions in BE-LDPE Filaments

Material	Function
Waste Vegetable Oil	Monomer
Isocyanate	Crosslinker
LDPE	Matrix

2.2 Testing

2.2.1 Visual and Microscopic Observation

The quantification of diameter and estimation of surface roughness were conducted using a Dino-Lite Digital Microscope with Dino-Capture 2.0 software and ImageJ. For each sample the reflection mode at 50× digital magnification. Image analysis was then performed using Image J software and average surface profiles were generated.

2.2.2 Thermal Analysis

To obtain detailed information about the effect of temperature on virgin LDPE and doped LDPE B3 emitted from tested printing materials, thermogravimetric analysis (TGA) was performed. A thermogravimetric analysis system (Model: LINSES) was connected to measuring devices for particle concentration and size distribution, including a Scanning Mobility Particle Sizer (SMPS) and a Condensation Particle Counter (CPC) (TSI Inc.). Six samples were used for laboratory testing, identical to the printing materials used for FDM. The tested filament samples were cylindrical in shape with a diameter of 1.75 mm and mass 2.0 milli gram ± 0.5 gram. These samples were subjected to thermal loading according to a prescribed temperature gradient scheme. The thermal analysis was performed from ambient temperature 35°C to 600°C over 60 minutes at a consistent heating rate of 10°C/min. Next Volatile Test was performed to evaluate the weight loss of material. The temperature was setup 110 °C and the initial weight sample was 0.5 milli gram ± 0.4 gram.

2.2.3 Mechanical Properties

To evaluate the mechanical properties five test specimens for each ratio include virgin LDPE as reference were prepared for each filament sample. The average value was calculated for every five samples and virgin. The tensile properties were measured following the ASTM D2256 standard using Universal Tensile Machine AG-I Shimadzu equipped with a 5 kN load cell. The gauge length of the test specimens was set to 100 mm, diameter filament was fixed to 1.75 mm ± 0.05 mm and the testing speed was maintained at 10 mm/min. The test was conducted at room temperature between 26 to 28 Celsius.

2.2.4 Morphology and Macroscopic Observation

The morphological analysis of the filament surface and cross-section was performed using a JEOL JSM-6380LA scanning electron microscope (SEM) at different magnifications (50×, 100×, and 200×). The cylindrical filaments were cut to a length of 10 mm and a diameter of 1.75 mm then coated with an ultrathin layer of platinum to ensure electrical conductivity.

2.3 Single Screw Extruder

The BE was first mechanically mixed with waste LDPE granules (size: 1-2 mm). The feedstock filament with a diameter of 1.75 ± 0.05 mm, was then produced using a single-screw compounder (Felfill Evo 3, maximum

barrel temperature: 300 ℃) by varying barrel temperature, screw speed, and pull speed, as shown in Table 2. The uniformity of the feedstock filaments was monitored within this range using a diameter sensor on the extruder. The image for machine extruder was illustrated in Fig. 2.

Table 2. Extruder process parameter.

Barrel Temperature (℃)	Screw Speed (rpm)	Pull Speed (rpm)	Fan Speed (rpm)
180	4	3.7	15

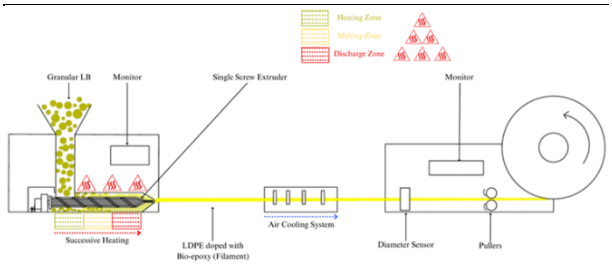

Fig. 2. Schematic Diagram for Physical Mixing Process.

2.4 Processing Method

The processing of LDPE with BE filaments begins with the preparation of the BE mixture. The process starts by combining waste vegetable oil (monomer) with isocyanate (crosslinker) in a 1:0.5 ratio. This liquid mixture is stirred thoroughly until a homogeneous solution is achieved, forming the BE. Upon solidification, the BE is manually mixed with LDPE granules (matrix) at room temperature through vigorous stirring to ensure uniform distribution of the functional filler. The pre-mixed composite is then allowed to cure at room temperature for several hours to enhance bonding and stability. The BE content is introduced at varying mass fractions, as shown in Table 3.

Table 3. Different percent of bio-polymer particle to produce polymer modification

Sample Name	Percentage BE (%)	Mass BE (g)	Mass LDPE (g)
Virgin LDPE	0	0	40
LB 1	1	0.4	40
LB2	2	0.8	40
LB3	3	1.2	40
LB4	4	1.6	40
LB5	5	2.0	40

The doped LDPE undergoes a degassed process to remove trapped air and prevent moisture. To further prevent the formation of air bubbles or pores during the extrusion process the coated LDPE is dried in an oven at 100°C for 24 hours in Memmert UNB 100 Oven before extrusion process.

Next, 40g doped LDPE is processed in a Brabender mixer at 180°C for 10 minutes to facilitate uniform distribution and partial crosslinking. During this process, the BE act as a functional filler dispersed into LDPE matrix promoting better interfacial adhesion. The controlled temperature and mixing time ensure that the material achieves a homogeneous distribution and preventing premature degradation. The resulting viscous melt LB is then collected and cooled before further processing into extrudates.

The result LB extrudates are collected and subsequently crushed and pelletized into uniform pellets with a diameter ranging from 1 to 5 mm. The palletization process ensures that the material is broken down into small manageable granules and improve flowability and melt consistency during the extrusion process.

The LDPE-BE pellets are fed into a single screw extruder Felfil Evo 3 where LB melted and extruded at a screw speed of 4 rpm and a temperature of 180°C. The filament diameter is monitored and controlled by a built-in sensor system ensures a consistent diameter of 1.75 mm ± 0.05 mm. After extrusion, the filament is cooled using an air-cooling system with speed fan 15 rpm to solidify its structure. It is then wound onto spools at a spool speed of 3.7 rpm, maintaining uniform tension and layering. Finally, 1-meter-long filaments are collected for storage, testing, and further characterization. The experimental setup is schematically illustrated in Fig. 3.

Fig. 3. Illustration of the LDPE-BE Composite Filament Fabrication Process.

3 RESULT

3.1 Physical Analysis

Fig. 4. shows filament diameter and surface characteristics were analyzed using a Dino-Lite digital microscope with a 50x magnification, allowing detailed observation of the filament's texture and uniformity. The measured diameters of the virgin LDPE and BE coated filaments (1%-5%) ranged from 1.70 mm to 1.75 mm, which falls within the acceptable 3D printing tolerance of 1.75 mm ± 0.05 mm (1.70 mm - 1.80 mm). This confirms that all filaments are dimensionally suitable for the printing process ensure proper extrusion through the nozzle 3D printer [17].

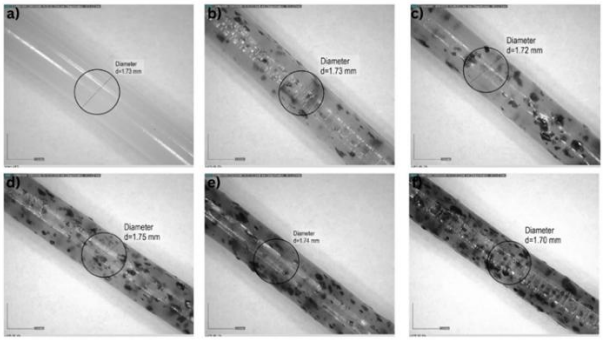

Fig. 4. Diameter determined with Dino Capture 2.0: Virgin LDPE (a): LDPE (b); LB 1% (c); LB 2% (d); LB 3% (e); LB 4% (f) and LB 5% filament samples.

Fig. 5 shows the surface roughness profile of LDPE filaments coated BE at different concentrations 1%-5% shows that the filament (gray line) is the smoothest, with minimal fluctuations in grayscale intensity. As BE concentration increases surface roughness generally rises with LB 1-3 (red, blue, green) exhibited moderate roughness while LB 4 (purple) and 5 (orange) display significant variations indicates rougher surfaces. The higher surface roughness in LB 5 is attributed to the presence of pores formed due to ductile fracture. In

contrast, the virgin LDPE sample underwent smooth surface preventing pore formation through stretching which resulted in lower surface roughness [18].

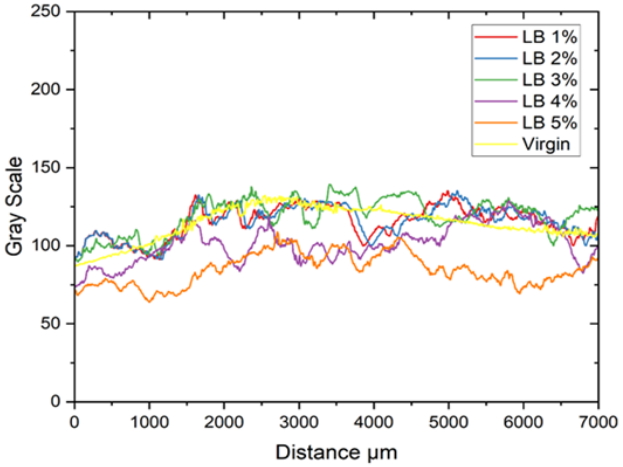

Fig. 5. Surface Roughness Profile of the Filament as Determined Using ImageJ.

3.2 Thermal Analysis

The thermal behavior of LDPE doped with BE was systematically investigated to evaluate its suitability for 3D printing applications. The first focus was on thermal stability and volatile release, which are critical for determining the material's performance during extrusion-based additive manufacturing (AM). These properties were analyzed using volatile content analysis and TGA, as presented in Fig. 6a and 6b, respectively.

Volatile content results (Fig. 6a) revealed that the total volatile content in LDPE-BE samples remained comparable to or slightly lower than that of virgin LDPE (2.40%), with LB 3 exhibiting the lowest volatile percentage (1.80%). This suggests that although volatilization begins earlier in the BE-modified samples, the overall amount of volatile matter is not significantly increased. The incorporation of BE introduced thermally sensitive compounds that begin to volatilize at lower temperatures, leading to early-stage weight loss due to the release of low molecular weight components.

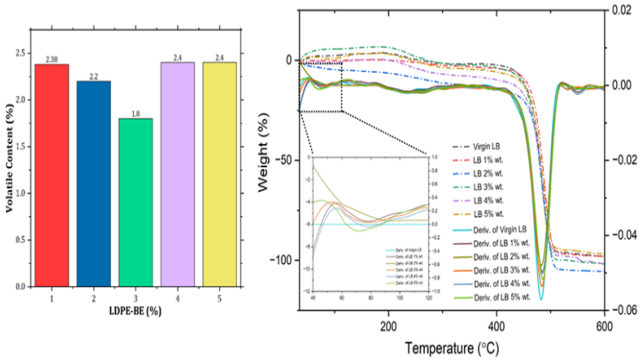

Fig. 6. Volatile Content of LDPE Doped Bio-Epoxy (a), Thermogravimetric Analysis (TGA) and Derivative Thermogravimetry (DTG) Curves of Virgin LDPE and LDPE-Bio-Epoxy Composites (b).

Thermogravimetric analysis (TGA) and its derivative (DTG) were conducted on virgin LDPE and LB 1–LB 5 filaments over the 30°C–800°C range under a nitrogen atmosphere, with the corresponding thermograms shown in Fig. 6b and data summarized in Table 4. The 5% weight loss temperature was slightly lower for LB (1–4) samples (180.24–184.58°C) compared to virgin LDPE (185.72°C), indicating an earlier onset of thermal degradation. However, LB 3 demonstrated the highest maximum degradation temperature (Tdmax = 486°C), indicates superior thermal resistance.

Table 4. Thermal Properties of Virgin LDPE and LDPE-Bio-Epoxy Composites.

Specs	Virgin LDPE	LB 1	LB 2 ;	LB 3	LB 4	LB 5
T_m (°C)	109	113	109	110	108	113
Td Max (°C)	484	483	482	486	485	483
Td Max (°C)	185.72	182.70	181.40	180.24	184.38	184.58
Td Max Remaining (%)	1.14	0.20	0.18	3.24	1.07	0.83

This enhanced stability in LB 3 is attributed to the formation of an efficient crosslinked network between isocyanate (-NCO) groups in the crosslinker and functional groups in the bio-epoxy, forming urethane (-NH–COO–) bonds. These interactions restrict polymer chain mobility, promote uniform filler distribution, and improve thermal resistance. As LDPE has limited reactive sites, the crosslinker plays a crucial role in creating additional chemical bonding, resulting in a more thermally stable structure. The residual mass at Tdmax further supports this: LB 3 retained 3.24%, while LB 1, LB 2, LB 4, and LB 5 showed greater degradation (0.18–1.07%). These findings suggest that a higher Tdmax enhances 3D printability by improving the material's heat resistance [19].

Additionally, the broadening of endothermic peaks in the BE-modified samples suggests a disruption in the crystalline domains. This morphological change can impact viscoelastic properties and flow behavior during extrusion. Virgin LDPE displayed a sharp melting peak an indicator of high crystallinity which enhances mechanical strength but may limit melt processability. In contrast, the modified samples, particularly those with optimal BE content, showed more balanced thermal transitions and crystallinity, which is beneficial for 3D printing applications.

In summary, for LB filaments to be suitable for 3D printing, the formulation must strike a balance between thermal stability, crystallinity, and printability. Virgin LDPE, with its high crystallinity and sharp melting peak, provides good thermal stability but may be prone to warping and poor interlayer adhesion during printing. As BE content increases, crystallinity tends to decrease, which enhances flexibility and interlayer adhesion but may reduce mechanical strength. Among the modified formulations, LB 1 showed the most disrupted crystalline structure, suggesting excessive disturbance to the LDPE matrix. In contrast LB 3 and 4 exhibited the best compromise maintaining reasonable crystallinity while improving flexibility and adhesion. If high crystallinity and thermal stability are the primary concerns, virgin LDPE or LB 2 would be more suitable. However, for optimal 3D print performance, LB 3 and 4 offers a better balance by promoting good melt flow behavior, providing moderate crystallinity for structural integrity, and reducing warping. On the other hand, LB 5 may reduce crystallinity excessively making the filament too soft and potentially compromising print quality. Overall,

LB 3 and 4 appears to be the most promising formulation for extrusion-based 3D printing applications offers enhanced processability without significantly sacrificing mechanical or thermal performance.

3.3 Mechanical Analysis

Table 5 shows the tensile test results for virgin LDPE and LDPE filaments coated with BE at different concentrations (1%-5%) reveal a correlation between BE concentration and tensile strength (TS). The virgin LDPE sample exhibits a maximum stress of 8.469 MPa with the highest elongation at break 275% indicate its ductile nature. As BE concentration increases, TS initially improves due to better interfacial adhesion but declines at higher concentrations due to poor dispersion and phase separation. The highest maximum stress of 8.819 MPa with a strain of 149.137% was observed in LB 3 representing a 4.14% enhancement in tensile strength compared to virgin LDPE. This improvement can be attributed to the effective stress transfer facilitated by electrostatic interactions between adjacent chitosan (CTS) chains through their amine functional groups [20]. The incorporation of BE led to enhanced load distribution within the matrix that reinforces the composite structure. The superior mechanical performance of the LDPE doped BE composite was primarily due to the homogeneous dispersion of high-aspect-ratio CTS particles within the LDPE matrix as shown in Fig. 5 can resulted in ultra-high interfacial adhesion and the formation of robust ionic bonds thereby improves the overall structural integrity of the material [21][22]. However, beyond 3%, TS begins to decrease with LB 4 shows a moderate stress of 8.015 MPa and LB 5 drop further to 7.738 MPa despite maintains a relatively high strain (171.055%).

Table 4. Mechanical properties of filaments.

Types of Filaments	Maximum Stress (MPa)	Strain (%)	Elongation Break (%)
Virgin LDPE	8.469	182.537	274.969
LB 1	7.917	77.598	166.880
LB 2	8.819	149.137	232.084
LB 3	8.015	164.277	173.507
LB 4	7.738	171.055	101.255
LB 5	7.917	77.598	166.880

As shown in Fig. 7 shows the mechanical properties for filament the surface irregularities were observed in the LB 5% composite reduced the effectiveness of stress transfer between the BE and LDPE matrix. Gaps and weak spots were created at the interface make the proper bonding between the materials more difficult. As a results stress was concentrated in these weak areas leading to localized failures and a reduced load-bearing capacity [23][24]. Additionally, the tensile strength of the composite was affected by the distribution and arrangement of BE within the matrix especially when BE was randomly dispersed which is weakened the overall structure. LB 1 and 2 exhibit lower TS values 7.756 MPa and 7.917 MPa, respectively due to weaker interfacial bonding. This trend suggests that while moderate BE concentrations around 3% enhance TS excessive BE leads to phase separation and stress concentration ultimately reducing mechanical performance.

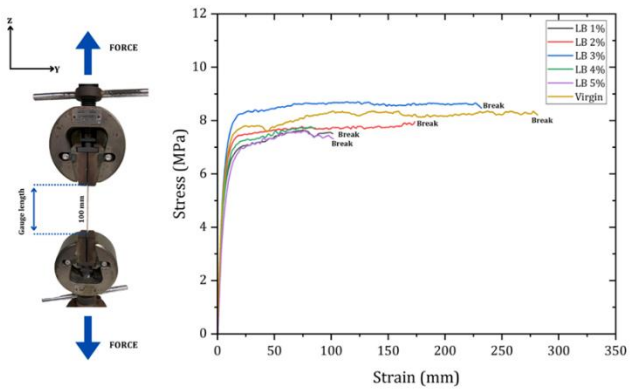

Fig. 7. Stress–strain curves for tensile test of 3D printing filament.

The mechanical characterization of LDPE filaments incorporated with BE demonstrates distinct performance trends. Minimal variability in maximum stress is exhibited, as evidenced by a low standard deviation of 0.434 MPa and a relative spread of 5.3%, as shown in Table 6. This suggests that the tensile strength of the LDPE matrix is not markedly compromised by the incorporation of BE across varying mass fractions. The consistency in maximum stress indicates that BE is effectively integrated within the polymer matrix, preserving the material's load-bearing capacity.

In contrast, strain and elongation at break parameters show substantially higher variability, with relative spreads of 34.9% and 39.6%, respectively, as shown in Table 5. This highlights that the presence and distribution of the BE phase are more significantly influencing ductility-related properties. The moderate dispersion in strain values implies that BE addition may induce either stiffening or plasticization effects, depending on the uniformity of dispersion and the quality of interfacial adhesion. The pronounced variation in elongation at break underscores the critical role of filler-matrix interactions, where inadequate dispersion or interfacial bonding facilitates premature failure, while homogeneous distribution enhances extensibility and toughness. Overall, it is suggested that while the mechanical strength of LDPE is largely retained upon BE incorporation, the ductility and fracture resistance are more significantly influenced by the morphology and distribution of the BE within the matrix.

3.4 Fractography Analysis

The fractography analysis could deliver more information about the failure modes of the filament specimens. The cross-sectional view of broken samples after tensile test was conducted to determine the failure mode of filament after it fracture as shown in Fig. 8. Fig. 8; (a-e) illustrates ridge markings, which indicate a substantial amount of energy dissipation during the damage process. These features are associated with a ductile fracture mechanism where significant plastic deformation occurs before failure. The presence of these ridges suggests that greater resistance to crack propagation is provided require a higher energy input for fracture progression [23]. Fig.8; (f) where smoother fracture surfaces with minimal plastic deformation are observed reflecting lower energy absorption before failures [25] [26].

The fracture morphology observed in the SEM images demonstrates a clear correlation between BE concentration 1% to 5% and the fracture behavior of

LDPE compared to virgin LDPE. As the BE concentration increases from 1% (image a) to 3% (image c) the material exhibits enhanced mechanical properties evidenced by the presence of elongated pores and extensive plastic deformation which indicates improved energy absorption during fracture [27]. This suggests that BE acts as a toughening agent by enhancing the polymer's ability to resist crack propagation. The optimal performance is observed at 3% BE (image c) where a balance between ductile and brittle fracture mechanisms is present as seen in the presence of cleavage facets, mist areas, and stable crack propagation. The transition of fracture behavior from the propagation zone to fatigue complete fracture is also depicted in this image reveal the number of microcrack is reduced.

However, beyond 3% bio-epoxy the fracture behavior shifts towards increased brittleness as seen in 4% and 5% BE (image d and e). At this concentration the material exhibits fewer elongated pores, increased cleavage facets, and shows the tear ridges indicates reduced ductility and higher susceptibility to brittle fracture [28]. In contrast, the virgin LDPE (image f) which contains no bio-epoxy, shows a smooth surface in polymer matrix. The types fractography in virgin LDPE shows with well-defined cleavage facets and no elongated pores demonstrate low energy dissipation and poor resistance to crack propagation [29][30]. The cleavage mark observed in this sample represents a low-energy fracture that propagated along well-defined low-index crystallographic planes known as cleavage planes [31].

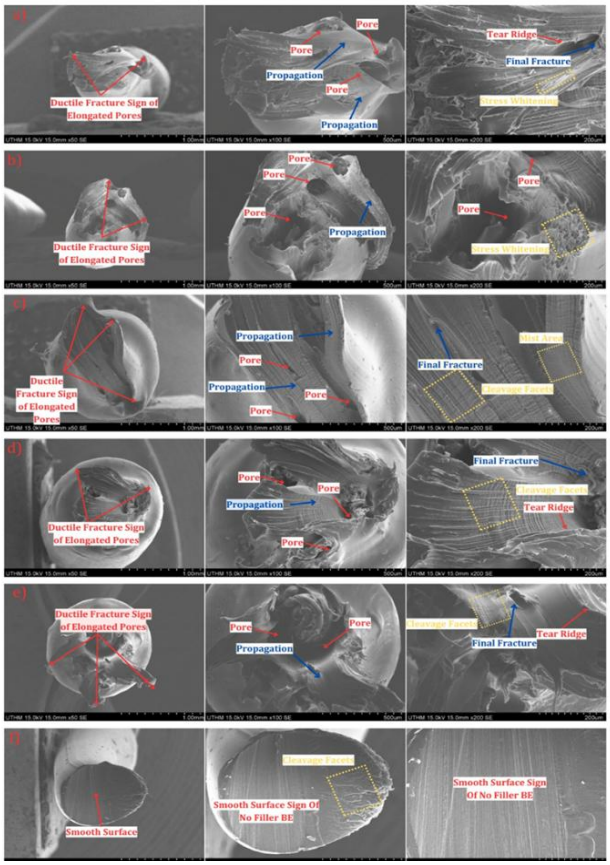

Fig. 8. SEM images at the magnification × 50, × 100, × 200, of the fractured surface of the filament a) LB b) LB 2%, c) LB 3%, d) LB 4%, e) LB 5% and f) Virgin LDPE.

3.5 Correlation Fractography and Thermal Analysis

The DSC and SEM analyses collectively highlight the relationship between thermal behavior, crystallinity, and mechanical properties in BE-modified LDPE. The DSC results in Fig. 6 shows that virgin LDPE has a sharp melting peak around 109-110°C indicates high crystallinity which corresponds to a more rigid structure. This sharp peak also suggests that the material is easy to degradation during thermal processing and its high crystallinity limits its processability make it less suitable for applications requiring easy melt flow. In the SEM images referred in Fig. 8 shows Virgin LDPE (image f) shows smooth fracture surfaces with well-defined cleavage facets reflecting a brittle fracture behavior with low energy dissipation consistent with the high crystallinity observed. As the BE concentration increases the DSC thermograms of BE-modified LDPE show slight shifts in melting temperature and broader endothermic peaks suggest a disruption in the crystalline structure. This disruption improves the material's flow behavior during processing particularly in 3D printing as the broader peaks indicate more gradual melting transitions. The SEM images support this, as lower BE concentrations (1-3%) exhibit ductile fracture features, such as elongated pores and significant plastic deformation, indicative of improved energy absorption. For instance, in image a (LB 1) and image c (LB 3) these ductile fracture features are prominent demonstrate enhanced toughness. At the optimal BE concentration of 3% (Fig. 8, image c) the DSC shows the increment melting temperature (110°C) reflecting a balance between crystallinity and toughness. SEM images at this concentration (image c) show a mix of ductile and brittle fracture mechanisms suggest that the material has both adequate toughness and thermal stability. However, beyond 3% BE, both the DSC and SEM reveal a shift towards brittleness. The broader DSC peaks indicate further disruption in crystallinity leading to reduced energy absorption and tougher fracture behavior. SEM images at these higher BE concentrations (4-5%) for example, in images d and e (LB 4 and LB 5) show fewer elongated pores and more cleavage facets indicates higher brittleness which is associated with the over-disruption of the crystalline structure. Thus, the sharp melting peak observed in the virgin LDPE's DSC thermogram shows in Fig. 6 correlates with its brittle fracture behavior in the SEM illustrates in Fig. 10 while the broader DSC peaks in BE-modified LDPE correspond to improved energy absorption and processing ease with the optimal BE concentration striking a balance between thermal stability and mechanical performance.

4 PRELIMINARY MECHANICAL RESULTS OF 3D PRINTING

The mechanical analysis of the polymer composite, as shown in Fig 9. a) demonstrates that the optimal performance is achieved at 3% Be content, where the material exhibits the highest stress 6.91 MPa and strain 37.8% indicates good interlayer bonding between matrix and fillers [32]. In Fig 10. b) the break force also peaks at 59.2 N at 3% Be further confirming this composition as the most mechanically robust. While displacement reaches a maximum at 4% Be 12.61 mm suggesting increased ductility, this comes at the expense of strength. Fig 10. c) illustrates the molecular mechanism behind these trends: at 3% Be, a well-balanced network of

hydrogen bonds, electrostatic bonds, and ion-dipole interactions is formed, leading to enhanced mechanical integrity. At lower Be content 1% and 2%), these interactions are insufficiently developed, and at higher content 4% and5% the bonding network becomes overloaded or disrupted. Therefore, 3% Be represents the ideal concentration, achieving the best combination of strength, elasticity, and structural cohesion in the polymer matrix.

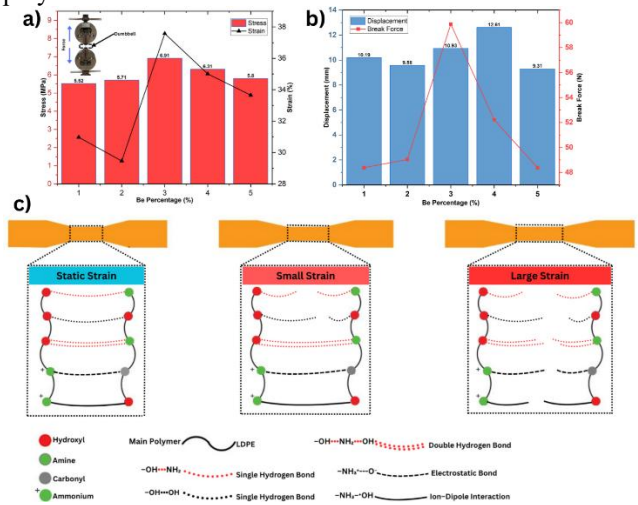

Fig. 9. Effect of Be Percentage on Mechanical Properties and Molecular Interaction Mechanism of Polymer Composites: (a) Stress and strain behavior under tensile testing at varying Be concentrations; (b) Displacement and break force data corresponding to Be percentage; (c) Schematic illustration of molecular bonding interactions.

5 CONCLUSION

The study investigates the incorporation of bio-epoxy as a functional filler in LDPE filaments to enhance their mechanical, thermal, and surface properties for 3D printing applications. The results indicate that a 3 wt% bio-epoxy concentration provides the most balanced improvement enhance tensile strength, interfacial adhesion, and thermal stability while minimizing issues related to agglomeration and stress concentration. Homogeneous dispersion of bio-epoxy improved stress transfer whereas excessive loading led to irregularities affecting adhesion and mechanical integrity. Thermal analysis confirmed that LDPE doped bio-epoxy composites exhibited improved stability with an optimal printing temperature identified before degradation. Additionally, surface roughness analysis emphasized the need for a controlled balance between smoothness and roughness to optimize printability. These findings highlight the potential of 3 wt% bio-epoxy as an optimal additive for LDPE-based 3D printing filaments offers enhanced performance and printability. Future research focus an advanced characterization techniques (e.g., in-situ rheology during extrusion, real-time thermal imaging) could elucidate how BE concentration (3–5%) influences melt flow and crystallization dynamics. To enhance sustainability, research must develop standardized recycling protocols for LDPE doped BE waste includes chemical/mechanical recycling efficiency and reprocessing effects on material properties. Finally, multi-functional composites (e.g., LDPE doped BE with nanoparticles or natural fibers) should be explored to expand applications in smart packaging, biomedical devices, and lightweight automotive components. These efforts would bridge the gap between lab-scale innovation and industrial adoption of bio-enhanced filaments.

ACKNOWLEDGEMENT

The research was supported by Universiti Tun Hussein Onn Malaysia (UTHM) through GPPS (vot Q826).

REFERENCES

Reference to a journal publication:

[1] S. A. S. Alali, M. K. M. B. J. Aldaihani, and K. M. Alanezi, “Plant Design for the Conversion of Plastic Waste into Valuable Chemicals (Alkyl Aromatics),” Applied Sciences (Switzerland), vol. 13, no. 16, Aug. 2023, doi: 10.3390/app13169221.

[2] S. Ghatge, Y. Yang, J. H. Ahn, and H. G. Hur, “Biodegradation of polyethylene: a brief review,” 2020. doi: 10.1186/s13765-020-00511-3.

[3] P. S. Eselem Bungu, K. Pflug, and H. Pasch, “Selectivity of Thermal Analysis in the Branching Analysis of Low Density Polyethylene,” Macromol Chem Phys, vol. 221, no. 12, 2020, doi: 10.1002/macp.202000095.

[4] P. B.A, L. N, A. Buradi, S. N, P. B L, and V. R, “A comprehensive review of emerging additive manufacturing (3D printing technology): Methods, materials, applications, challenges, trends and future potential,” Mater Today Proc, vol. 52, pp. 1309–1313, 2022, doi: 10.1016/j.matpr.2021.11.059.

[5] T. Pereira, J. V. Kennedy, and J. Potgieter, “A comparison of traditional manufacturing vs additive manufacturing, the best method for the job,” in Procedia Manufacturing, Elsevier B.V., 2019, pp. 11–18. doi: 10.1016/j.promfg.2019.02.003.

[6] C. H. Lee, F. N. B. M. Padzil, S. H. Lee, Z. M. A. Ainun, and L. C. Abdullah, “Potential for natural fiber reinforcement in pla polymer filaments for fused deposition modeling (Fdm) additive manufacturing: A review,” 2021. doi: 10.3390/polym13091407.

[7] V. Mishra, S. Negi, S. Kar, A. K. Sharma, Y. N. K. Rajbahadur, and A. Kumar, “Recent advances in fused deposition modeling based additive manufacturing of thermoplastic composite structures: A review,” 2023. doi: 10.1177/08927057221102857.

[8] X. Zhang, W. Fan, and T. Liu, “Fused deposition modeling 3D printing of polyamide-based composites and its applications,” 2020. doi: 10.1016/j.coco.2020.100413.

[9] N. Verma, P. Awasthi, A. Gupta, and S. S. Banerjee, “Fused Deposition Modeling of Polyolefins: Challenges and Opportunities,” 2023. doi: 10.1002/mame.202200421.

[10] A. Karaki, A. Hammoud, E. Masad, M. Khraisheh, A. Abdala, and M. Ouederni, “A review on material extrusion (MEX) of polyethylene - Challenges, opportunities, and future prospects,” Jul. 24, 2024, Elsevier Ltd. doi: 10.1016/j.polymer.2024.127333.

[11] D. Tang, F. H. Marchesini, L. Cardon, and D. R. D’hooge, “State of the-Art for Extrudate Swell of Molten Polymers: From Fundamental Understanding at Molecular Scale toward Optimal Die Design at Final Product Scale,” 2020. doi: 10.1002/mame.202000340.

[12] A. Karaki, E. Masad, M. Khraisheh, and M. Ouederni, “Fused deposition modeling of polyethylene (PE): Printability assessment for low-density polyethylene and polystyrene blends,” Composites Part C: Open Access, vol. 15, Oct. 2024, doi: 10.1016/j.jcomc.2024.100499.

[13] R. Hsissou et al., “New epoxy composite polymers as a potential anticorrosive coatings for carbon steel in 3.5% NaCl solution: Experimental and computational approaches,” Chemical Data Collections, vol. 31, Feb. 2021, doi: 10.1016/j.cdc.2020.100619.

[14] R. Hsissou et al., “Evaluation of corrosion inhibition performance of phosphorus polymer for carbon steel in [1 M] HCl: Computational studies (DFT, MC and MD simulations),” Journal of Materials Research and Technology, vol. 9, no. 3, pp. 2691–2703, 2020, doi: 10.1016/j.jmrt.2020.01.002.

[15] O. Dagdag et al., “Epoxy resins and their zinc composites as novel anti-corrosive materials for copper in 3% sodium chloride solution: Experimental and computational studies,” J Mol Liq, vol. 315, Oct. 2020, doi: 10.1016/j.molliq.2020.113757.

[16] H. S. Abdo, I. A. Alnaser, A. H. Seikh, J. A. Mohammed, S. A. Ragab, and A. Fouly, “Ecofriendly Biochar as a Low-Cost Solid Lubricating Filler for LDPE Sustainable Biocomposites: Thermal, Mechanical, and Tribological Characterization,” Int J Polym Sci, vol. 2023, 2023, doi: 10.1155/2023/2445472.

[17] C. D. B. Comprado et al., “Fabrication, Testing and Statistical Analysis of a Project-Based Single-Screw Filament Extruder,” in 2021 IEEE International Conference on Automatic Control and Intelligent Systems, I2CACIS 2021 - Proceedings, 2021. doi: 10.1109/I2CACIS52118.2021.9495872.

[18] R. Kumar, R. Singh, V. Kumar, P. Kumar, C. Prakesh, and S. Singh, “Characterization of in-House-Developed Mn-ZnO-Reinforced Polyethylene: A Sustainable Approach for Developing Fused Filament Fabrication-Based Filament,” J Mater Eng Perform, vol. 30, no. 7, 2021, doi: 10.1007/s11665-021-05801-5.

[19] H. Liu, S. Chen, H. Y. Mi, Y. Wang, C. Liu, and X. Wang, “High strength microcellular thermoplastic polyimide/carbon fiber composite foams containing flexible ether amine, rigid diaminodiphenyl ether, and triaminopyrimidine moieties: Synthesis and fabrication,” Chemical Engineering Journal, vol. 496, Sep. 2024, doi: 10.1016/j.cej.2024.154384.

[20] M. Roszowska-Jarosz et al., “Mechanical properties of bio-composites based on epoxy resin and nanocellulose fibres,” Materials, vol. 14, no. 13, 2021, doi: 10.3390/ma14133576.

[21] S. N. Sarmin et al., “Enhancing the properties of date palm fibre reinforced bio-epoxy composites with chitosan – Synthesis, mechanical properties, and dimensional stability,” J King Saud Univ Sci, vol. 35, no. 7, 2023, doi: 10.1016/j.jksus.2023.102833.

[22] Zhao, C., Wang, Y., Tang, G., Ru, J., Zhu, Z., Li, B., Guo, C. F., Li, L., & Zhu, D. (2022). Ionic Flexible Sensors: Mechanisms, Materials, Structures, and Applications. In Advanced Functional Materials (Vol. 32, Issue 17). https://doi.org/10.1002/adfm.202110417

[23] K. Senthilkumar, M. Chandrasekar, M. Jawaid, H. Fouad, and B. Abu-Jdayil, “Enhancing the Bio-epoxy Composites with Oil Palm Fibre as Reinforcement: Assessment of Mechanical, Physical and Thermal Properties,” J Polym Environ, Nov. 2024, doi: 10.1007/s10924-024-03359-6.

[24] Xu, B., Li, Y., Wang, S., Luo, H., & Lu, B. (2022). Study on the strength characteristics and failure characteristics of the composite load-bearing structure in the cemented filling field. Construction and Building Materials, 330. https://doi.org/10.1016/j.conbuildmat.2022.127242

[25] M. R. Ayatollahi, A. Nabavi-Kivi, B. Bahrami, M. Yazid Yahya, and M. R. Khosravani, “The influence of in-plane raster angle on tensile and fracture strengths of 3D-printed PLA specimens,” Eng Fract Mech, vol. 237, 2020, doi: 10.1016/j.engfracmech.2020.107225.

[26] C. Li, Y. Piao, B. Meng, Y. Hu, L. Li, and F. Zhang, “Phase transition and plastic deformation mechanisms induced by self-rotating grinding of GaN single crystals,” Int J Mach Tools Manuf, vol. 172, 2022, doi: 10.1016/j.ijmachtools.2021.103827.

[27] X. Zhang, H. Hao, R. Tian, Q. Xue, H. Guan, and X. Yang, “Quasi-static compression and dynamic crushing behaviors of novel hybrid re-entrant auxetic metamaterials with enhanced energy-absorption,” Compos Struct, vol. 288, 2022, doi: 10.1016/j.compstruct.2022.115399.

[28] Su, H., Toda, H., Masunaga, R., Shimizu, K., Gao, H., Sasaki, K., Bhuiyan, M. S., Uesugi, K., Takeuchi, A., & Watanabe, Y. (2018). Influence of hydrogen on strain localization and fracture behavior in Al–Zn–Mg–Cu aluminum alloys. Acta Materialia, 159. https://doi.org/10.1016/j.actamat.2018.08.024

[29] W. Li et al., “Tough Hydrogels with Isotropic and Unprecedented Crack Propagation Resistance,” Adv Funct Mater, vol. 32, no. 43, 2022, doi: 10.1002/adfm.202207348.

[30] WANG, Y., WANG, X., LIU, Z., LIU, S., WANG, S., CHEN, H., SONG, C., BAI, Y., WANG, P., & LIU, Y. (2022). A plastic strain energy method exploration between machined surface integrity evolution and torsion fatigue behaviour of low alloy steel. Chinese Journal of Aeronautics, 35(10). https://doi.org/10.1016/j.cja.2021.11.003

[31] G. Yin et al., “Effects of the metal-ceramic continuous transition region on the tensile strength and crack propagation behavior of 8YSZ/CoNiCrAlY coating,” Surf Coat Technol, vol. 481, 2024, doi: 10.1016/j.surfcoat.2024.130630.

[32] Ali, M. H., Kurokawa, S., Shehab, E., & Mukhtarkhanov, M. (2023). Development of a large-scale multi-extrusion FDM printer, and its challenges. International Journal of Lightweight Materials and Manufacture, 6(2). https://doi.org/10.1016/j.ijlmm.2022.10.001